CHAPTER II
LITERATURE REVIEW

In this section, an overview of AMS is presented, followed by a discussion of its development and the ongoing efforts to downsize AMS systems. The functions of key electrostatic components in the ion beamline, including the octupole deflector and Einzel lens, are explained. Additionally, the design of the Heatwave Labs ionizer and the calibration of the heating filament's power consumption are described. Finally, Maxwell's equations relevant to particle-tracking simulations in CST Studio Suite are introduced.

2.1 Accelerator Mass Spectrometry (AMS)

AMS is a sensitive and robust technique typically applied to the quantification of long-lived radioisotopes in samples too small to be decay-counted (Marchetti et al., 2005). Mass spectrometers (Haag, A. M., 2016) comprised of three main components: an ion source, a mass analyzer, and a detector. AMS for radiocarbon dating is an advanced technique for determining the age of biological samples by finding the proportion of the radioisotope of ^{14}C to ^{12}C in graphite form. While the conventional technique determines the age of a sample by counting the radioactivity of ^{14}C (β-minus decay reaction). In comparison (Harris, 1987), the AMS technique, which directly measures the ratio of ^{14}C to ^{12}C atoms, allows for faster and more accurate analysis of samples with very low quantities of graphite (Seema S. Ojha, 2013). showed that minimum sample size is thus reduced approximately 1000-fold (from 1 g to 1 mg), and the datable time span of the method can, theoretically, be doubled (from 40,000 to 80,000 years).

2.2 Development of AMS

The development of AMS has seen significant advancements over the decades, particularly in terms of downsizing the system. Initially, AMS systems required large, high-energy accelerators with terminal voltages in the range of MeV (Mega-electron volts), such as the systems seen at Japan Atomic Energy Agency Accelerator Mass Spectrometry facility at Tono (JAEA-AMS-TONO) as shown in Figure 2.1, which utilized terminal voltages of 4.5 MV or higher (Matsubara et al., 2014).

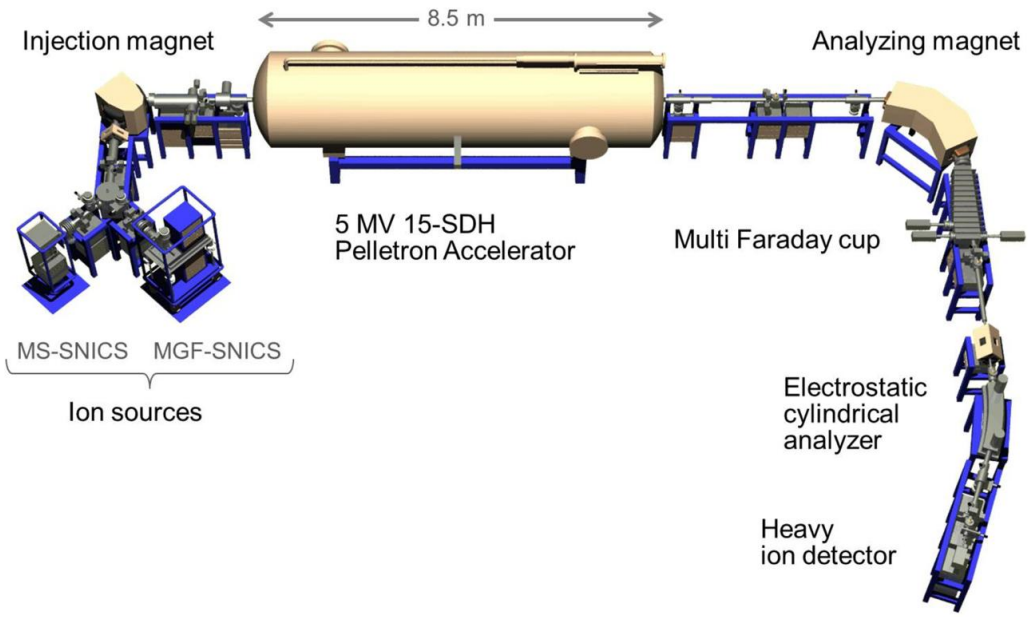

Figure 2.1 The layout of AMS system at Japan Atomic Energy Agency Accelerator Mass Spectrometry facility at Tono (JAEA-AMS-TONO) (Matsubara et al., 2014).

These large systems were effective in providing high-precision isotopic measurements but were costly, required significant space, and involved complex operational demands. However, in recent years, advancements in technology have enabled the development of compact AMS systems that operate at much lower terminal voltages, typically around 200 kV. An example of this innovation is the Mini Carbon Dating System (MICADAS), a compact AMS setup that achieves high performance despite its smaller size. With overall dimensions of just 2.5 x 3 m^2 as shown in Figure 2.2, MICADAS integrates all essential components, including a high-voltage power supply and vacuum system, into a highly compact footprint.

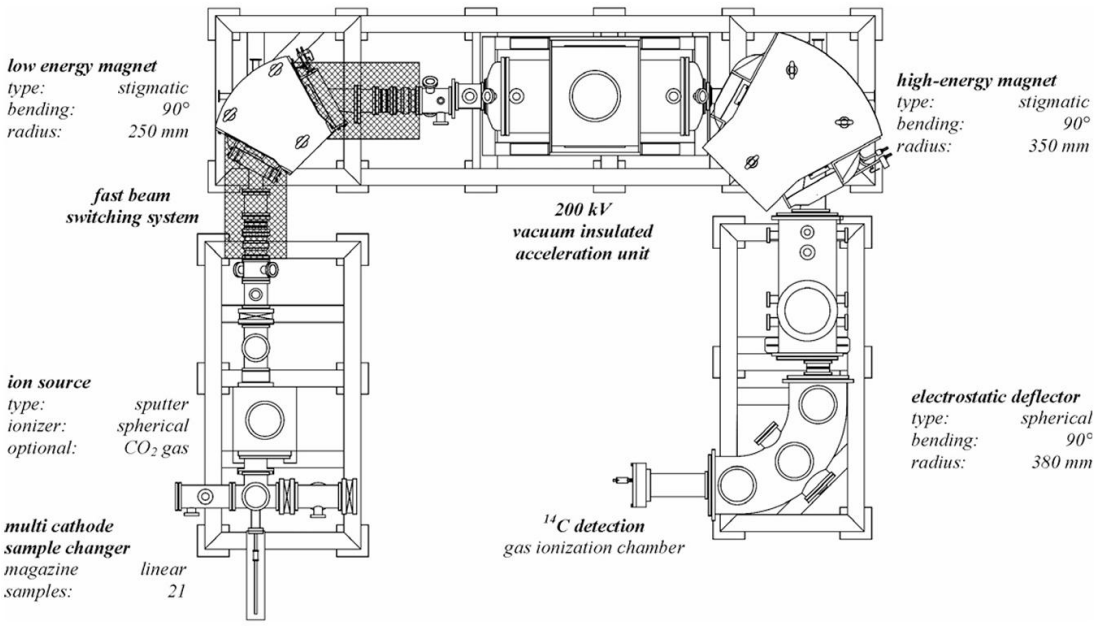

Figure 2.2 The layout of MICADAS. With its small dimensions of 2.5 x 3 m^2, can be easily fit into a common laboratory environment (H.-A. Synal et al., 2007).

The system as shown in Figure 2.2 operates at 200 kV, significantly reducing the size and complexity without compromising precision. These improvements have made AMS systems more accessible and affordable, allowing smaller laboratories and institutions to utilize the technology for applications in radiocarbon dating, environmental research, and archaeology.

In the sample preparation, the AMS system for radiocarbon dating requires the use of negative carbon ions, which are produced by the Source of Negative Ions by Cesium Sputtering (SNICS). This negative ion source designed for extracting negative carbon ions in graphite form by cesium sputtering. For this reason, there are various methods for the sample preparation and the compression method of graphite into the sample holder. The paper by Balsley et al. (1987) details methods for converting carbonaceous materials into solid graphite suitable for use in a cesium sputter ion source. Initially, carbon samples are converted to carbon dioxide, which is then reduced to graphite powder using hydrogen and iron as a catalyst. The graphite powder, or amorphous carbon, is encapsulated in a tantalum tube, compressed at high pressure (around 14 kbar), and heated to approximately 2500°C in a vacuum. This process ensures the formation of a smooth, hard graphite surface, which is ideal for producing high-intensity ion beams with good

geometrical characteristics. The preparation method emphasizes consistency, minimal contamination, and reproducibility, making it crucial for accurate AMS measurements. Moreover (Broek TAB, Roberts ML, 2024), the Ion Plus AG (MICADAS) demonstrated that recessed targets, particularly at a 1 mm depth, produced a more narrowly focused beam with lower emittance, improving transmission through the accelerator. Small graphite samples (200 µg) with recessed surfaces generated higher currents for longer periods, resulting in a 2–3X increase in ionization efficiency. Additionally, isotopic ratio measurements of these samples were more stable over time. Due to these benefits, the standard method for pressing MICADAS graphite has been updated to include a recessed surface approach.

2.3 Mini Carbon Dating System (MICADAS)

MICADAS is a highly compact and energy-efficient ^{14}C-AMS instrument designed for routine radiocarbon measurements. The heart of MICADAS is a hybrid cesium sputter ion source capable of producing stable negative-ion currents of 50–150 µA for solid graphite cathodes and 10–20 µA for gas samples (≥10 µg C). A random-access sample changer holds up to 40 graphite or gas cathodes, allowing continuous operation without breaking vacuum or cooling down the ion source.

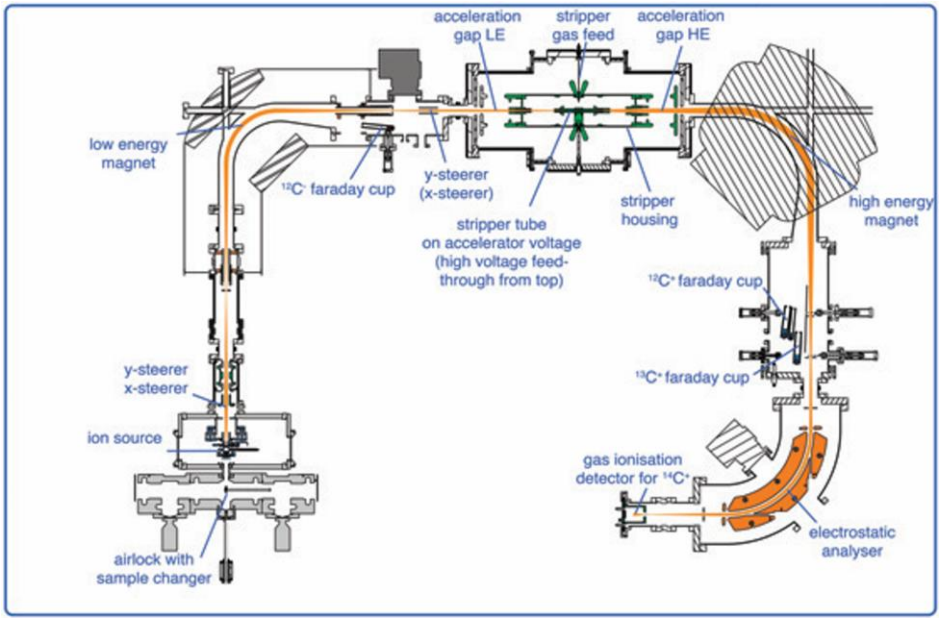

Figure 2.3 Simplified diagram of the ion optics of the MICADAS system. The high-voltage segment is shown in green (Synal et al., 2007).

Ion acceleration to 200 kV is provided by a vacuum-insulated solid-state power supply, eliminating the need for SF_6 or other insulating gases. Downstream of the accelerator, helium stripping yields up to 47 % transmission of ^{14}C ions, with background levels (machine blanks) extending beyond 68,000 radiocarbon years. A low-noise gas ionization detector then identifies ^{14}C ions with high reliability, enabling routine dating of samples older than 50,000 radiocarbon years.

Operation of MICADAS requires only 2.5 kW of average power and is fully air-cooled, so no water cooling is needed. The vacuum system including the ion source region, accelerator terminal, and analysis beamline must maintain pressures in the ultra-high vacuum (UHV) range (10^{-7} to 10^{-8} torr) to minimize scatter and background. Continuous monitoring of vacuum levels is achieved through integrated gauges, and automated vacuum interlocks protect both the ion source and the accelerator during sample changes or shutdowns.

Key specifications and operational conditions of MICADAS include:

- Ion source: Hybrid cesium negative-sputter, 40 position sample wheel
- Negative-ion currents: 50–150 µA (solid); 10–20 µA (gas, ≥10 µg C)
- Accelerator: 200 kV vacuum-insulated solid-state power supply
- Stripping medium: Helium (≤47 % ^{14}C transmission)
- Detector: Gas ionization detector with low noise, enabling blank levels > 68,000 ^{14}C yr BP
- Power consumption: ≤2.5 kW (air-cooled)
- Footprint: 3.2 m × 2.6 m × 2.2 m; weight ≈ 4,500 kg
- Sample throughput: Automated magazine changes allow continuous measurement without breaking vacuum.

By integrating all high-voltage components into a vacuum-insulated terminal and using permanent magnet technology, MICADAS minimizes infrastructure needs no SF_6 or water cooling is required and delivers fast tuning, long-term measurement stability, and minimal maintenance. This makes it particularly attractive for laboratories aiming to perform high-precision ^{14}C dating with limited space and resources

2.4 Electrostatic deflector

The misalignment of the beamline components can cause the beam to deviate from the axis; therefore, an electrostatic deflector is required to correct the beam trajectory. This device utilizes electric fields to alter the path of charged particles. When ions pass through a region with an electric field, they experience a force proportional to the field strength and the charge of the ions. Electrostatic deflectors typically consist of parallel plates (Spivak-Lavrov et al., 2023) or electrodes with a voltage difference applied between them. Quadrupole deflectors are generally more suitable for applications requiring basic focusing and steering, where linear beam dynamics dominate. In contrast, octupole deflectors are advantageous in scenarios where the correction of non-linear effects is critical, such as in high-precision beam shaping and stability enhancement.

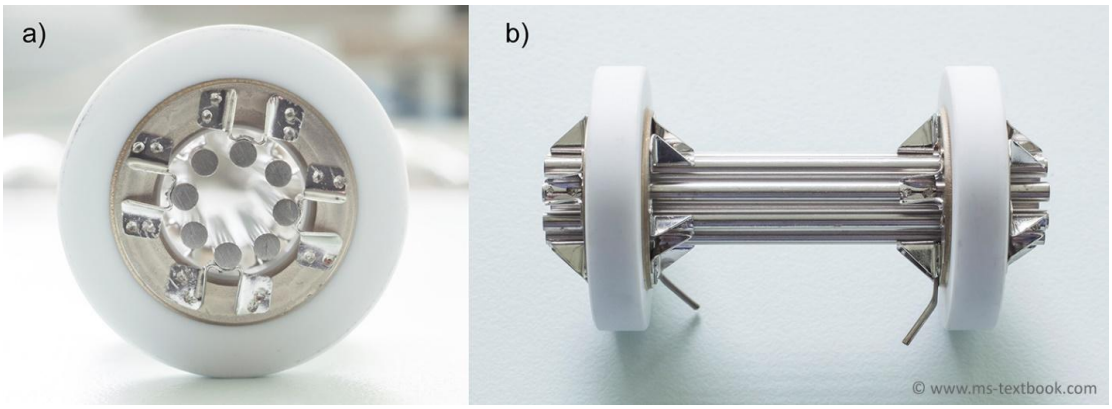

Figure 2.4 Octupole deflector: (a) Head-on view showing the octupole alignment, and (b) side view. Ref. MS-Textbook. (n.d.). For instructors.

Drummond, I. W. (1984) explains that an octupole is a type of multipole ion optical element consisting of eight rods or electrodes arranged symmetrically around the beam path. Its primary function is to apply corrective forces to ion beams, particularly in systems where beam shaping and the correction of higher-order aberrations are critical. Unlike simpler devices, such as quadrupoles, which correct second-order effects, the octupole addresses higher-order aberrations, making it useful for fine-tuning the beam's profile, especially in high-precision systems such as ion microscopy or mass spectrometry. By adjusting the voltages applied to the rods, the octupole compensates for distortions and imperfections in the beam, improving overall beam quality and stability. It is often used in combination with other optical elements, such as quadrupoles or Einzel lenses, to refine the beam shape and correct asymmetries in the beam trajectory.

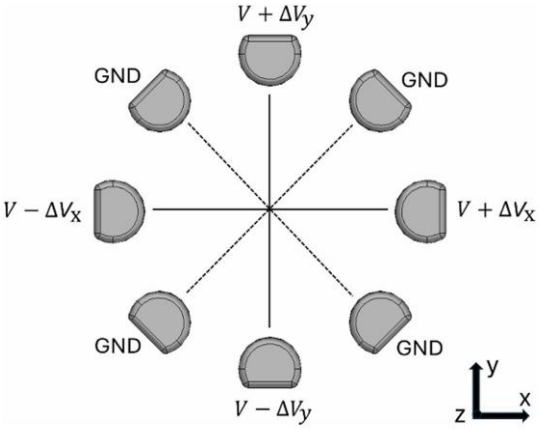

Figure 2.5 The schematic design of the octupole deflector (Chomchan et al., 2024).

The paper (Chomchan et al., 2024) designed and simulated a simple electrostatic octupole deflector intended for use in a compact AMS devoted to radiocarbon dating. The deflector is positioned immediately downstream of a cesium-sputter ion source and consists of eight stainless-steel rod electrodes arranged symmetrically in a 40 mm circular aperture. By biasing the horizontal and vertical electrode pairs independently (ΔV_x and ΔV_y), the authors demonstrated through finite-element electric-field analysis and charged-particle tracking (using CST Studio Suite) that the beam can be steered in the X and Y directions without cross-coupling.

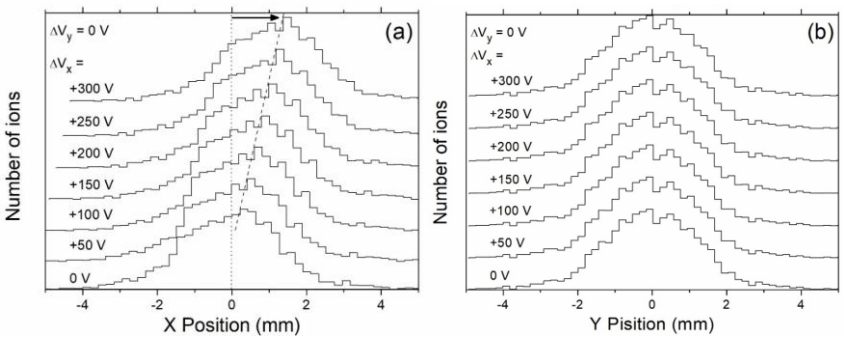

Figure 2.6 The horizontal (a) and vertical (b) profiles of a 40 keV C^- beam horizontally deflected with ΔV_y set to zero, while ΔV_x is varied from 0 to +300 V (Chomchan et al., 2024).

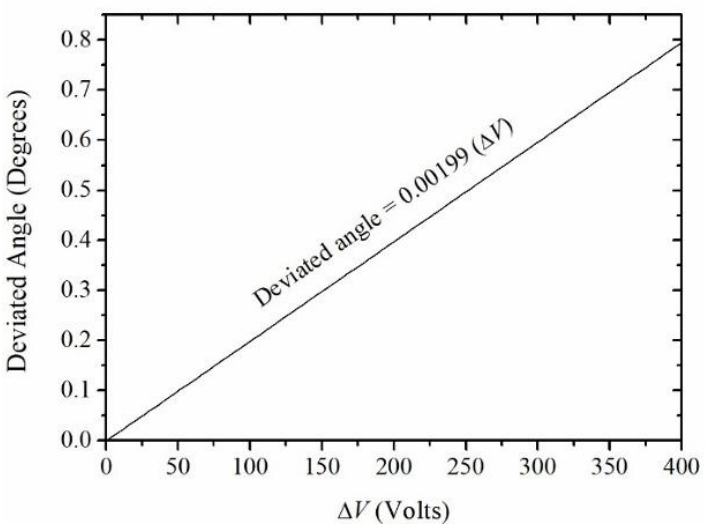

Figure 2.7 The simulated deviated angle of a 40 keV C^- beam after passing through the deflector as a function of ΔV (Chomchan et al., 2024).

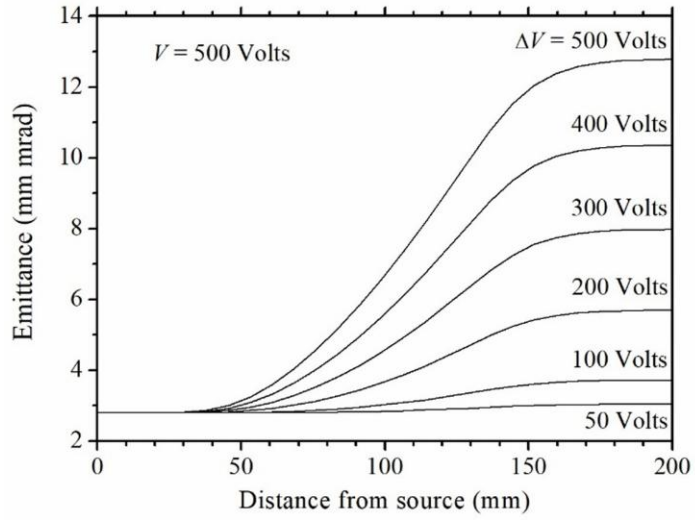

Figure 2.8 The emittance of the 40-keV C^- beam entering the deflector at 40 mm from source (Chomchan et al., 2024).

Simulations showed a linear relationship between the applied voltage difference and the beam's deflection angle, and that the emittance of a 40 keV C^- beam increases with larger deviation angles (e.g., from 2.9 mm·mrad unperturbed to approximately 6.0 mm·mrad at ΔV ≈ 200 V for a 0.4° deviation). These results confirm that beam deflections in the two directions are independent, with virtually no coupling. The emittance of the deviated beam increases with increasing deviated angle, thus the adjusting voltage.

2.5 Electrostatic lens

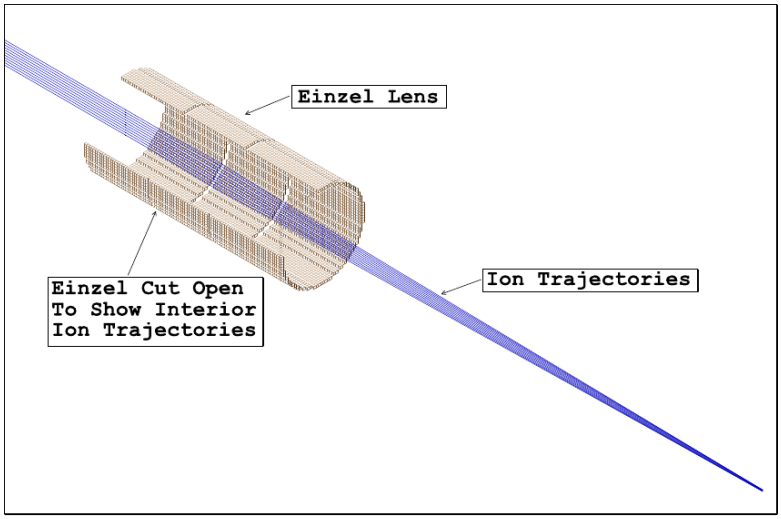

Figure 2.9 Cutaway view of ion trajectories in an Einzel lens. Ref. Scientific Instrument Services, Inc. (n.d.). SIMION: User Manual - Chapter 2: Ion Optics and Electrostatic Fields.

An Einzel lens is a type of electrostatic lens used in charged particle beam systems, such as ion and electron beamlines, to focus the beam without significantly altering its energy. It consists of three cylindrical electrodes, with the outer two typically grounded and the middle one held at a specific voltage. When a charged particle beam passes through the lens, the electrostatic field created by the potential difference causes the beam to focus by adjusting its trajectory. What makes the Einzel lens particularly useful is that it focuses the beam while maintaining the initial energy of the particles, making it ideal for applications where energy stability is crucial, such as AMS and other precision ion optics systems. Its simple design and effectiveness at controlling beam divergence and focusing make it a vital component in many particle accelerator setups.

Park et al. (2020) presents a simulation analysis of ion beam extraction using an electrostatic Einzel lens for low-energy AMS. The research focuses on optimizing beam focusing and separation in a compact AMS system. The SIMION program was used to simulate the ion trajectories, revealing that the use of an Einzel lens enhances the focusing and separation of ion beams, improving transmission efficiency.

The study evaluated the lens in two operational modes, accel-decel and decel-accel , as shown in Figure 2.11a and 2.11b and found that while both modes successfully transmitted the ion beam, they had different effects on beam emittance and isotopic separation. The decel-accel mode was found to be better suited for beam injection into an accelerating column or analyzing isotopic separation, while the accel-decel mode was more advantageous for other low-energy ion transport systems.

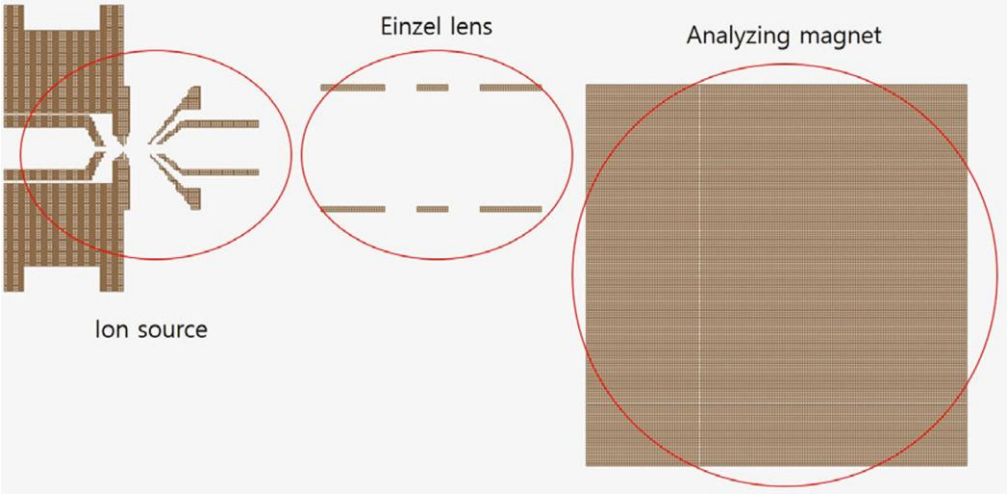

Figure 2.10 Geometry of the ion source, electrostatic Einzel lens, and analyzing magnet implemented via the SIMION code (Park et al., 2020).

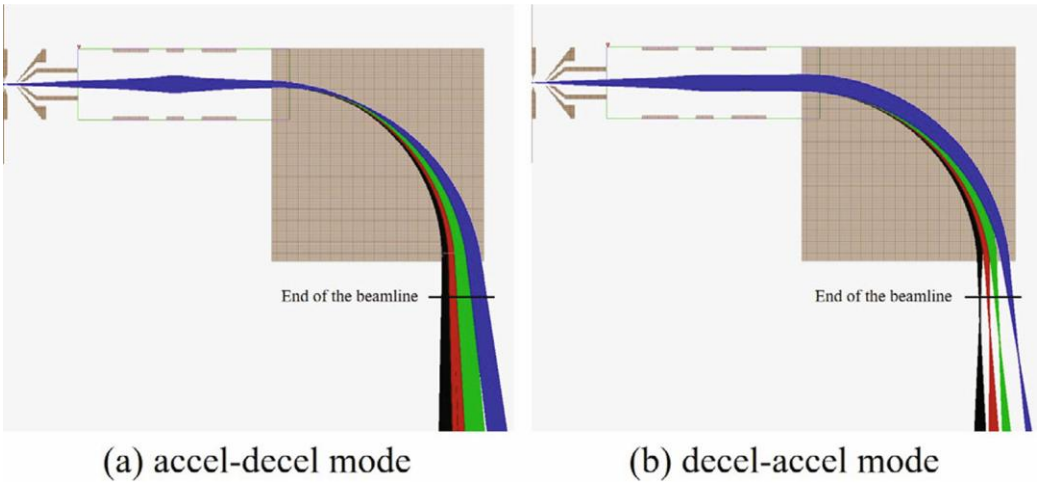

Figure 2.11 Simulation results for beam transmission in two different modes of the Einzel lens: (a) accel-decel mode and (b) decel-accel mode (Park et al., 2020).

Suethonglang et al. (2024) present the design and simulation of a compact electrostatic Einzel lens tailored for use in a low-energy (40 keV) carbon ion beamline within an AMS. The lens consists of three coaxial cylindrical electrodes, each with a 35 mm inner diameter, 3 mm wall thickness, and 17 mm axial gap, mounted inside a standard 4-inch vacuum tube. The two outer electrodes are held at ground potential, while the central electrode is biased either positively or negatively to generate the focusing field.

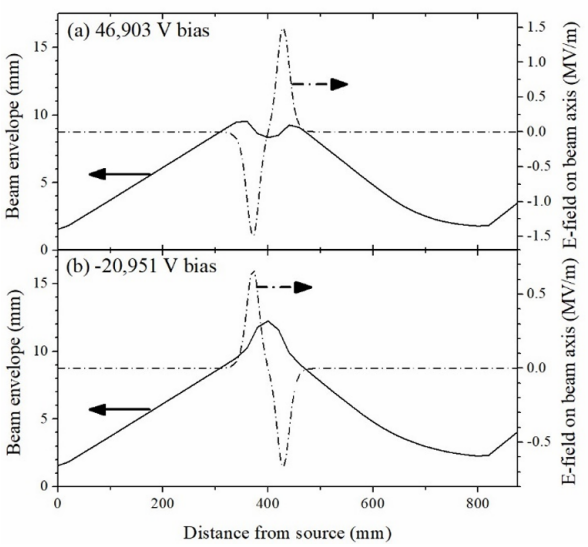

Figure 2.12 The ion beam envelope and electric field component on the beam axis beam when the electrostatic Einzel lens was biased with (a) 46,903 V and (b) -20,951 V (Suethonglang et al., 2024).

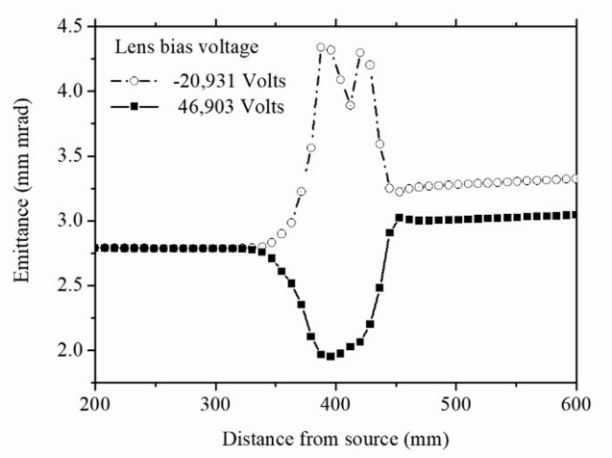

Figure 2.13 The emittance of the ion beam when the ES Einzel lens was biased with (a) 46,903 V and (b) -20,951 V (Suethonglang et al., 2024).

Using CST Studio Suite for particle-tracking simulations, the authors optimized the bias voltage and electrode dimensions. They found that a negative bias of –20,951 V on the middle electrode produced a tighter focus and lower emittance growth (an ~18 % increase from 2.8 mm·mrad to ~3.3 mm·mrad) compared to a positive bias of +46,903 V (where emittance rose to ~3.2 mm·mrad at the waist) as shown in Figure 2.13.

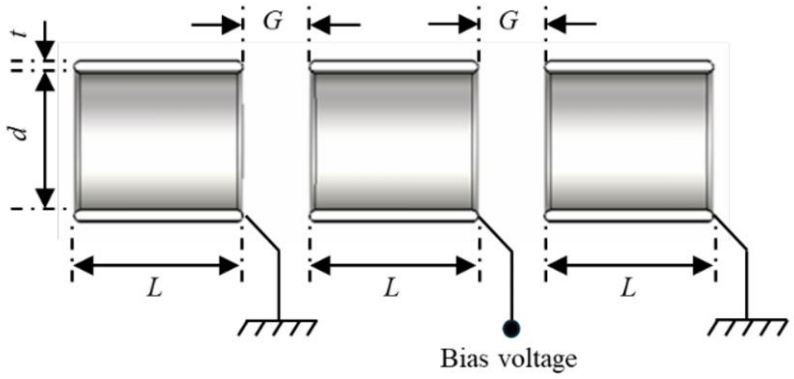

Figure 2.14 Cross-sectional drawing of an electro-static Einzel lens with three cylindrical tube electrodes (Suethonglang et al., 2024).

Moreover, by varying the length of the middle electrode from 43 mm to 86 mm, they demonstrated that the longer middle electrode minimized downstream emittance while still fitting within the 4-inch chamber. Specifically, at twice the side-tube length (relative length = 2.0), beam emittance at the focus (800 mm from the ion source) was lowest (~3.15 mm·mrad) when the optimized negative bias (≈ –21,500 V) was applied. In conclusion, the optimized Einzel lens focuses a 40 keV C^- beam to a waist at 800 mm from the source with a demagnification factor of 1.0 and only a ~12.5 % emittance increase. This design combines high beam quality with practical high-voltage resilience, making it well-suited for a compact AMS system.

2.6 Heater for ionizer

For ion beam production inside the cesium sputter source, an ionizer is required to ionize the cesium vapor into cesium ions (Cs^+).

2.6.1 Design of the ionizer from HeatWave Labs, Inc.

In the negative carbon ion production section, a cesium sputter ion source requires an ionizer heated to 1200 ℃ to convert cesium vapor into cesium ions for sputtering against the graphite at the sample cathode. HeatWave Labs, Inc. has developed an ionizer specifically tailored to these requirements, as shown in Figure 2.15.

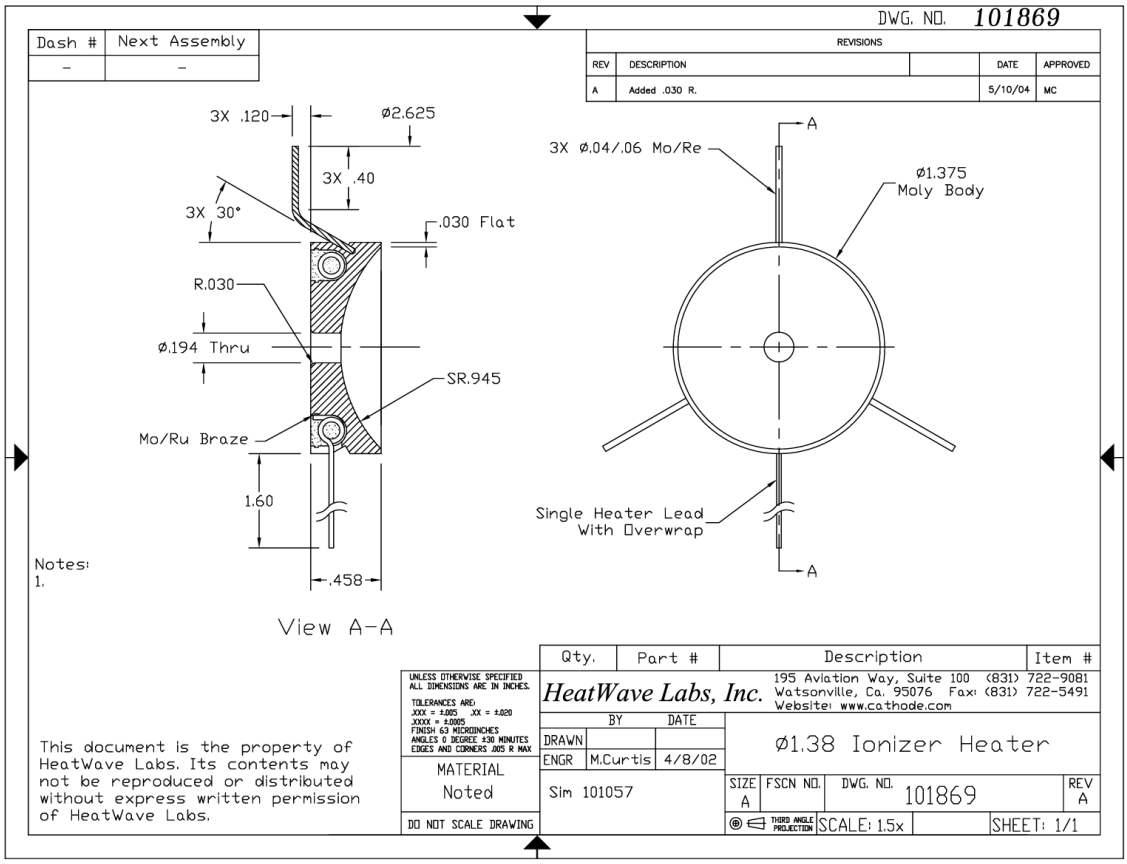

Figure 2.15 Drawing of the Ø1.38-inch ionizer heater from HeatWave Labs, Inc. Ref. Cathode Engineering Co. (2025). HeatWave Labs, Inc. Cesium-Sputter Ionizer Heater (Ø1.38″) Product Data Sheet.

They also performed a calibration of power consumption and voltage at various temperatures as shown in Table 2.1 and provided all dimensions and material specifications. The ionizer body is made of molybdenum (Mo), and the heating filament is made of molybdenum-rhenium (MoRe). The ionizer has a diameter of 1.38 inches

Table 2.1 Power Consumption of the Ionizer Heater at Different Temperatures (IonPlus AG) Ref. Cathode Engineering Co. (2023). HeatWave Labs AG Cesium-Sputter Ionizer Product Data Sheet.

Temperature (°C)	V (Volt)	Current (A)	Power (Watt)
1,000	6.16	12.22	72.28
1,110	7.8	14.06	109.67
1,210	9.5	15.8	150.1

2.6.2 Properties of MoRe alloy

MoRe (Molybdenum-Rhenium alloy) is commonly used as a filament material for the ionizer in cesium sputter sources due to its high melting point, excellent resistance to high temperatures, and stable electrical properties. It can withstand the high heat required for thermionic emission, making it ideal for generating electrons to ionize cesium in vacuum environments. Additionally, MoRe resists corrosion from cesium and maintains stability under vacuum conditions, ensuring long-lasting performance and reliable ionization efficiency. These properties make it an optimal choice for high-performance ion sources in sputtering applications.

Table 2.2 Mechanical, Physical, Electrical, and Thermal Properties of MoRe Alloy Ref. Rhenium.com. (n.d.). Molybdenum-Rhenium Alloy Annealed Properties.

Molybdenum-Rhenium Alloy, Annealed | MECHANICAL AND PHYSICAL PROPERTIES

	Metric	English
Physical Properties		
Density	13.5 g/cc	0.488 lb/in^3
Mechanical Properties		
Tensile Strength, Ultimate	1180 MPa	171000 psi
	240 MPa	34800 psi
	@Temperature 1200 °C	@Temperature 2190 °F
	620 MPa	89900 psi
	@Temperature 800 °C	@Temperature 1470 °F
Tensile Strength, Yield	845 MPa	123000 psi
	210 MPa	30500 psi
	@Temperature 1200 °C	@Temperature 2190 °F
	415 MPa	60200 psi
	@Temperature 800 °C	@Temperature 1470 °F
Elongation at Break	22%	22%
Modulus of Elasticity	365 GPa	52900 ksi
Poissons Ratio	0.285	0.285
Shear Modulus	132 GPa	19100 ksi
Electrical Properties		
Electrical Resistivity	0.0000220 ohm-cm	0.0000220 ohm-cm
Critical Superconducting Temperature	10.9 K	10.9 K
Thermal Properties		
CTE, linear	5.72 µm/m-°C	3.18 µin/in-°F
	@Temperature 500 °C	@Temperature 932 °F
	6.45 µm/m-°C	3.58 µin/in-°F
	@Temperature 1000 °C	@Temperature 1830 °F
Thermal Conductivity	36.8 W/m-K	255 BTU-in/hr-ft^2-°F
Melting Point	2450 °C	4440 °F
Maximum Service Temperature, Air	725 °C	1340 °F
Component Elements Properties		
Molybdenum, Mo	52.50%	52.50%
Rhenium, Re	47.50%	47.50%

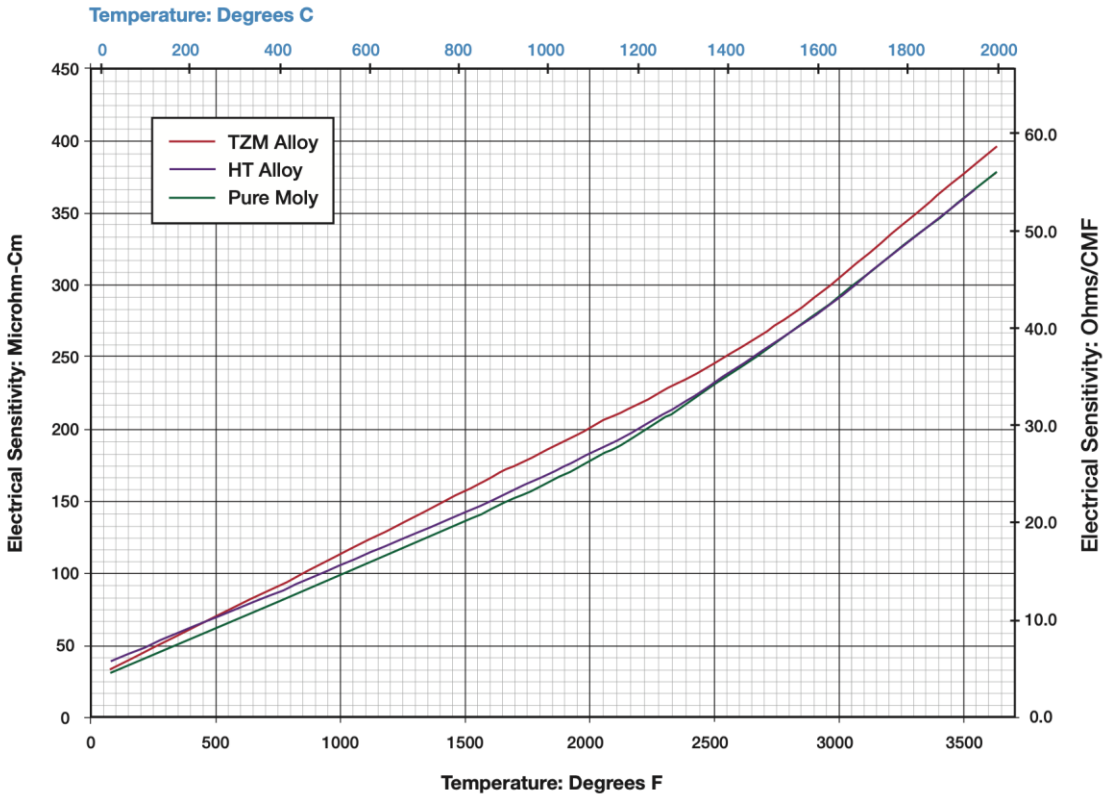

Figure 2.16 Electrical Resistivity of TZM Alloy, HT Alloy, and Pure Molybdenum vs. Temperature Ref. National Element Industries. (2017). Molybdenum Technical Data.

This Figure 2.16 shows how the electrical resistivity of three molybdenum-based materials TZM alloy (red), HT alloy (blue), and pure molybdenum (green) increase almost linearly with temperature from room temperature up to about 2,000 °F (≈1,090 °C). At 2,200 °F (≈1,205 °C), resistivity reaches roughly 200 μΩ·cm (≈30 Ω/CMF) for all three, with TZM consistently exhibiting the highest values and pure molybdenum the lowest. The close spacing of the curves indicates that alloying with Ti, Zr, or heat treatments modifies resistivity only slightly across this temperature range. As the temperature of these molybdenum-based materials increases, their electrical resistivity rises accordingly because lattice vibrations (phonons) intensify, scattering conduction electrons more frequently and impeding their flow. As a result, at higher filament temperatures such as the 1,200 °C needed for cesium sputtering the ionizer heater's resistance will be significantly higher than at room temperature, requiring greater voltage or current to maintain the same power level.

2.7 Particle tracking solver in CST Studio Suite

Particle Tracking Solver is a submodule of Particle Studio that applies the Lorentz force law to fields computed from Maxwell's equations in this case via finite element analysis (FEA) to update particle positions and velocities over discrete time steps. First, CST's FEM or FIT field solvers perform FEA to solve Maxwell's equations and generate detailed electric and magnetic field maps throughout the geometry. The core equations used in CST Studio Suite's Particle Tracking Solver then couple the particle's equation of motion (the Lorentz force law) with those pre-computed FEA fields, allowing accurate tracking of charged particles through complex electromagnetic structures.

2.7.1 Finite element analysis

In CST Studio Suite, Finite Element Analysis (FEA) is primarily used to compute electromagnetic fields within complex geometries. The FEA solver automatically generates a high-quality tetrahedral mesh that conforms to the model's surfaces and internal features, with adaptive refinement in regions of high field gradient or geometric detail.

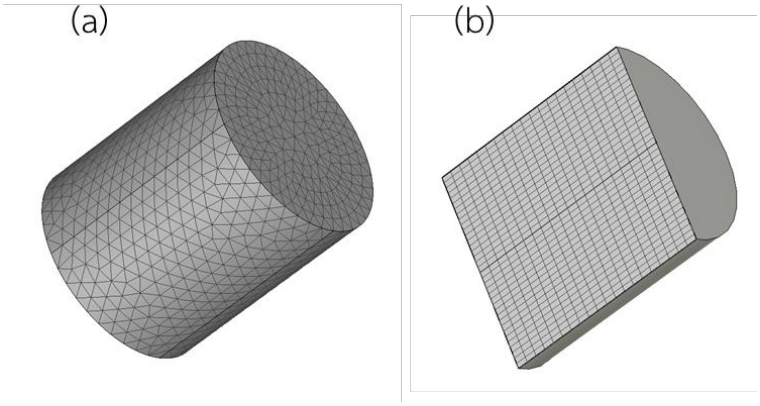

Figure 2.17 Mesh types for computer simulation. (a) Tetrahedral mesh (b) Hexahedral mesh.

Once the mesh is generated by CST's Mesher (via Mesh ⟶ Global Properties or Mesh View ⟶ Update), a static field solver discretizes Poisson's equation (together with material relations) on that mesh to produce an electrostatic (and, if required, magnetostatic) field map. This solver supports both hexahedral and tetrahedral grids. The resulting $\mathrm{E}(\mathrm{r})$ and $\mathrm{B}(\mathrm{r})$ distributions are then exported to Particle Studio's Tracking Solver, which integrates the Lorentz force law through these static fields—updating each particle's trajectory over time.

2.7.2 Equation of motion (Lorentz force law)

A charged particle with charge q and mass m moves according to the Lorentz force law:

$$\frac{d\mathbf{p}}{dt} = q(\mathbf{E} + \mathbf{v} \times \mathbf{B}) \quad \text{Eq. 1}$$

Where,

$\mathbf{p}$ is the relativistic momentum of the particle,

$\mathbf{E}(\mathbf{r}, t)$ is the electric field at position $\mathbf{r}$ and time t,

$\mathbf{B}(\mathbf{r}, t)$ is the magnetic field at position $\mathbf{r}$ and time t,

$\mathbf{V}$ is the particle's velocity.

For a relativistic particle, momentum is given by:

$$\mathbf{p} = \gamma m\mathbf{v}, \text{ with } \gamma = \frac{1}{\sqrt{1-\frac{|\mathbf{v}|^2}{c^2}}} \quad \text{Eq. 2}$$

Thus, the full relativistic form of the equation of motion becomes:

$$\frac{d}{dt}(\gamma m\mathbf{v}) = q(\mathbf{E} + \mathbf{v} \times \mathbf{B}). \quad \text{Eq. 3}$$

The particle position is then updated by:

$$\frac{d\mathbf{r}}{dt} = \mathbf{v} \quad \text{Eq. 4}$$

2.7.3 Maxwell's equations

CST's Particle Tracking Solver first computes $\mathbf{E}$ and $\mathbf{B}$ throughout the simulation domain by solving Maxwell's equations (in differential form) using the Finite Integration Technique (FIT):

2.7.3.1 Gauss's law (Electric)

$$\nabla \cdot \mathbf{D} = \rho\,, \quad \text{where} \quad \mathbf{D} = \varepsilon \mathbf{E} \qquad \text{Eq. 5}$$

2.7.3.2 Gauss's law for magnetism

$$\nabla \cdot \mathbf{B} = 0\,, \quad \text{where} \quad \mathbf{B} = \mu \mathbf{H} \qquad \text{Eq. 6}$$

2.7.3.3 Faraday's law

$$\nabla \times \mathbf{E} = -\frac{\partial \mathbf{B}}{\partial \mathrm{t}} \qquad \text{Eq. 7}$$

2.7.3.4 Ampère - Maxwell law

$$\nabla \times \mathbf{H} = \mathbf{J} + \frac{\partial \mathbf{D}}{\partial \mathrm{t}} \qquad \text{Eq. 8}$$

Where ρ is the free charge density and $\mathbf{J}$ is the conduction current density.